



UNIVERSITÀ POLITECNICA DELLE MARCHE  
Repository ISTITUZIONALE

Comparative fragility methods for seismic assessment of masonry buildings located in Muccia (Italy)

This is the peer reviewed version of the following article:

*Original*

Comparative fragility methods for seismic assessment of masonry buildings located in Muccia (Italy) / Chieffo, N.; Clementi, F.; Formisano, A.; Lenci, S.. - In: JOURNAL OF BUILDING ENGINEERING. - ISSN 2352-7102. - STAMPA. - 25:(2019), p. 100813. [10.1016/j.jobe.2019.100813]

*Availability:*

This version is available at: 11566/267525 since: 2022-05-25T11:17:31Z

*Publisher:*

*Published*

DOI:10.1016/j.jobe.2019.100813

*Terms of use:*

The terms and conditions for the reuse of this version of the manuscript are specified in the publishing policy. The use of copyrighted works requires the consent of the rights' holder (author or publisher). Works made available under a Creative Commons license or a Publisher's custom-made license can be used according to the terms and conditions contained therein. See editor's website for further information and terms and conditions.

This item was downloaded from IRIS Università Politecnica delle Marche (<https://iris.univpm.it>). When citing, please refer to the published version.

(Article begins on next page)

# Comparative fragility methods for seismic assessment of masonry buildings located in Muccia (Italy)

Nicola Chieffo<sup>1</sup>, Francesco Clementi<sup>2</sup>, Antonio Formisano<sup>3</sup>, Stefano Lenci<sup>4</sup>

<sup>1</sup>Department of Civil Engineering, Politehnica University of Timișoara, Romania

<sup>2,4</sup> Department of Civil Engineering, Construction and Architecture,

Polytechnic University of Marche

<sup>3</sup>Department of Structures for Engineering and Architecture, University of Naples “Federico II”

<sup>1</sup>nicola.chieffo@student.upt.ro, <sup>2</sup>francesco.clementi@univpm.it, <sup>3</sup>antoform@unina.it, <sup>4</sup>lenci@univpm.it

## Abstract

The current paper focuses on a sector of the historic centre of Muccia, in the district of Macerata (Italy), affected by the seismic sequence that involved Central Italy in 2016. *The main goal is the comparison in terms of fragility curves among two vulnerability assessment methodologies, empirical and mechanical ones.* The study area has been structurally and typologically identified according to the Building Typology Matrix (BTM). The physical vulnerability analysis of the urban-sector was performed through the application of a specific form for masonry building aggregates. Consecutively, an isolated masonry building, damaged after the seismic sequences, has been selected as a case study. On the assessed building, empirical fragility curves are presented according to the Guagenti & Petrini's correlation law. Furthermore, the numerical model was built by using the macro-element approach, in order to simulate the seismic behaviour of the analysed structure. Mechanical properties of masonry were defined according to the New Technical Codes for Constructions (NTC18), assuming a limited knowledge level (LC1). A refined mechanical fragility functions have been derived and compared to the empirical ones.

From the results achieved, the empirical method tends to overestimate by 5% and 10% the expected damage for slight and moderate thresholds. Contrary, for PGA values greater than 0,3g the damage levels decreased by 30% and 20%, with reference to the near collapse and collapse conditions, respectively.

**Keywords:** Masonry buildings, empirical method, mechanical method, vulnerability assessment, damage scenarios, fragility curves.

## 1. State of Art

The seismic risk assessment is a multivariate problem based on the estimation of three major factors such as vulnerability (V), hazard (H) and exposure (E). The combination of these factors allows to qualitatively and quantitatively describe the risk in a given area and allows estimates of possible losses as a result of catastrophic events. The estimation of these three factors is very important for the planning of interventions (on an urban scale) of risk mitigation [1, 2]. The concept of vulnerability, V, is mainly based on the capacity of a building to suffer specific damage due to a seismic event. The exposure, is connected to the nature, quantity and value of the properties and activities of the area that can be influenced directly or indirectly by a seismic event and finally, the hazard is understood as the probability of occurrence of the asymptomatic event of a certain intensity in a specific site, and depends mainly on the geographic position and the geological characteristics of the site in which the event is expected. The seismic hazard represented by the frequency and the force of the earthquakes that affect it, or by its seismicity. It is defined as the probability that in an area and in a certain time interval an earthquake occurs that exceeds a threshold of intensity, magnitude or peak acceleration (PGA).

Masonry has been one of the most popular construction materials developed during the centuries as it provided economic and functional solutions worldwide. Nevertheless, the existing unreinforced masonry buildings (URM) are typically identified as "*potential risk factors*" due to the behaviour of masonry that is very complicated to be predicted. In fact, when the URM buildings are subjected to shaking due to the earthquake, the mass of the walls and lightweight flexible diaphragms, leads to a rigid-fragile global behavior that triggers the possible collapse mechanisms increasing the possibility of repercussions on society (physical and economic losses). Generally, these constructions have been designed to resist only gravity loads, offering a very low resistance to seismic actions [3, 4].

The URM response depends on several aspects that mainly affect the ductility piers and strength of the walls [5]. The failure mode is affected by several parameters, such as the vertical compression due to gravity loads, the wall aspect ratio, the boundary conditions, and the relative strength between mortar joints and units. In the past, strong earthquakes have caused considerable damage given the poor consistency of the building samples. The damage is attributed to an inadequate structural integrity and to the lack of connection between the orthogonal walls which results in typical shear cracking and disintegration of the walls with consequent partial or total collapses [6, 7]. It seems evident that the many uncertainties, mainly associated with the mechanical characteristics of the basic material (not homogeneous and anisotropic) and construction techniques, negatively influence the structures' capacity to overcome a seismic event [8].

119 Focusing on historical centers, they are characterized by numerous buildings of immeasurable  
120 architectural and cultural value. In fact, the large number of old masonry buildings in many of the  
121 Italian seismic areas represents one of the crucial points for the preservation and protection of the  
122 existing heritage.

123 The heterogeneity of buildings formed in aggregate is a very delicate aspect as it requires a significant  
124 level of knowledge on every single building that is however very small compared to numerical  
125 analysis methodologies. Nevertheless, ordinary buildings located in the historical centres are often  
126 made of different quality masonries and constructive details that can highlight deficiencies with  
127 respect to safety conditions against seismic actions [9, 10]. A significant number of proposals based  
128 on simplified modeling approaches is already available in the scientific literature. Most of them are  
129 based on the assumption that the masonry wall is represented as a set of one-dimensional macro-  
130 elements (piers and spandrels), connected by nodes in such a way as to reproduce the behavior of the  
131 wall by an equivalent frame, which gives the possibility of using conventional numerical methods of  
132 structural mechanics [11, 12]. Other advanced methods, proposed in [13, 14], investigate the seismic  
133 response by means of non-linear dynamic analysis assuming that masonry behaves as a damaging-  
134 plastic material with almost vanishing tensile strength. Generally, the presence of vulnerability factors  
135 is a fundamental feature that significantly decreases the strength of the walls, influencing the damage  
136 distribution mainly due to out-of-plane actions. Furthermore, it has been stated that a preliminary  
137 structural assessment through kinematic limit analysis on partial failure mechanisms may be reliable  
138 only after a proper estimation of the different structural elements playing a role in the horizontal  
139 behavior (e.g. interlocking between walls, typology of masonry, distribution of horizontal loads,  
140 constraints and dead loads distribution, etc.). The comparison between the numerical results and the  
141 damage survey showed that the numerical approach used in [15] may be an adequate tool to properly  
142 evaluate the seismic response of historical masonry buildings. However, it would be unreasonable to  
143 perform numerical analyses on each individual building within historic centers.

144 To this purpose, the large-scale evaluation methodologies are mainly based on observational data for  
145 a significant sample of buildings, therefore, for the evaluation of the seismic vulnerability of the  
146 aggregates, rapid methods are generally used (vulnerability index method) for an appropriate  
147 vulnerability estimate and the attribution of the vulnerability class is supported on information on  
148 buildings (drawings and on-site inspections) [13, 14]. The peculiarity of this methodology lies in the  
149 fact that it can be combined with the macroseismic method for the assessment of damage scenarios.  
150 The macroseismic methodology, therefore, foresees to be able to evaluate the susceptibility of a stock  
151 of buildings to the variation of the hazard which in the specific case is defined as macroseismic

intensity EMS-98 [15]. The possibility of identifying the most vulnerable sample of buildings, allows previously to mitigate the effects of the seismic phenomenon [16].

Based on these premises, the main target of this research work is to identify the seismic response of the isolated building by means of fragility curves developed using different approaches in order to obtain a synthetic damage parameter under different grade earthquakes.

## **2. Historical background of the City of Muccia**

The City of Muccia (Fig.1) is an Italian town of 911 inhabitants in the province of Macerata in the Marche region. The Municipality is 454 m on the sea level with an area of 25.91 Km<sup>2</sup>. On the banks of the Chienti River, located at an important road junction since antiquity, Muccia hosts numerous archeological finds, remarkable 15<sup>th</sup> century churches and a wonderful Franciscan hermitage, oasis of peace and meditation. Since prehistory, has been characterised as a knot of important communication channels. In the middle Ages, under the name of Mutia, it was a strategic place for the processing and trade of grains, so that the lordship of Da Varano di Camerino erected a castle in defense of mills [17].



Figure 1. The city of Muccia in the Marche region of Italy.

On January 1436 it was sacked by the troops of Francesco Sforza when he occupied the Marche. His proximity to Camerino makes him presumptuous. Next, with the Napoleonic Kingdom of Italy, was part of the department of Tronto, district of Camerino, canton of the same name. With the district of Camerino, he passed to the Musone department in 1811. The definitive destruction of the Musone took into account decree no. 118 of July 14<sup>th</sup> 1807, and brought together in a single municipality several nearby locations, so that none of them had a population of less than 1000 inhabitants. During the Restoration, it was common under the governorate of Camerino, in the homonymous delegation. The advent of the Unity of Italy, the commune became part of the province of Macerata in Camerino's mandate. Muccia is also a center characterized by numerous archeological finds and sites of interest, among which are the Church of Santa Maria di Varano, with an octagonal plan, the "Tower of Massa", "Torraccia" at Mentori.s.l.m. 808 at Massaprofoglio (Fig. 2).





(a)



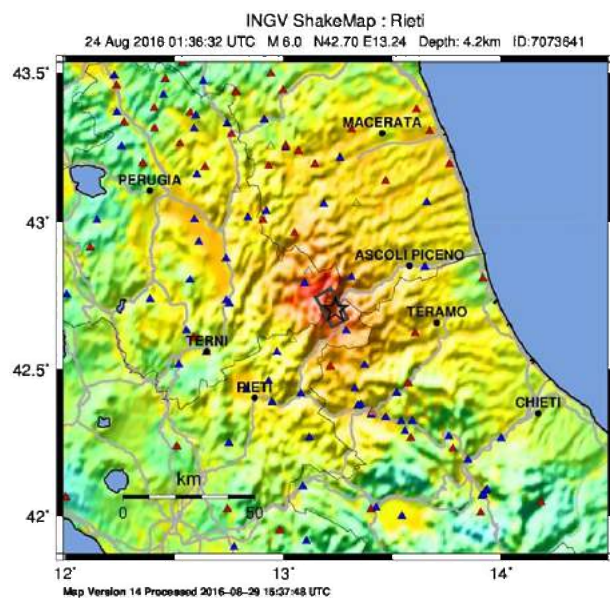
(b)

Figure 2. Archeological site: a) Sant Maria di Varano Church; b) Massaproglio Castle.

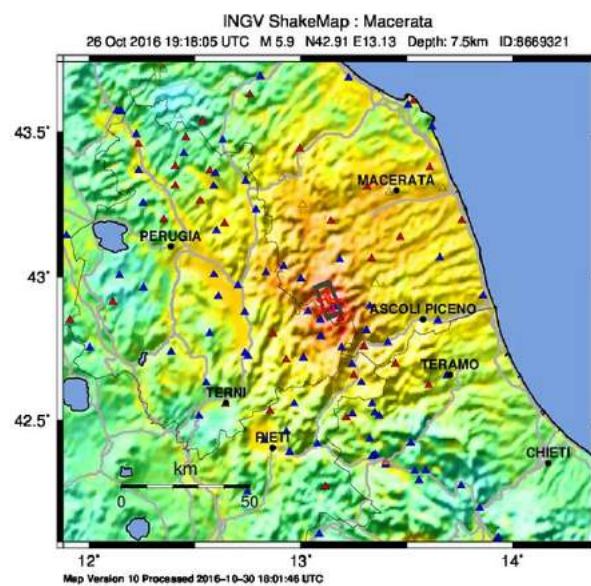
## 2.1. The Central Italy seismic sequences

The first main-shock occurred August 24<sup>th</sup>, 2016 had its epicenter in the province of Rieti (near the municipality of Accumoli), but it also affected the provinces of Perugia, Ascoli Piceno, L'Aquila and Teramo. The municipalities closest to the epicenter are: Accumoli, Amatrice, Arquata del Tronto. The maximum moment magnitude recorded,  $M_w$ , was equal to 6,0. The area affected by the aftershocks, which in a first approximation represents the extension of the activated fault, is approximately 25 km and is aligned in the sense NNO - SSE. Subsequently, several aftershocks have been recorded, the largest of which are in the area of Norcia (PG) with magnitude equal to 5,4. The hypocenter depths of the replicas are modest, almost all within the first 10 km [18].

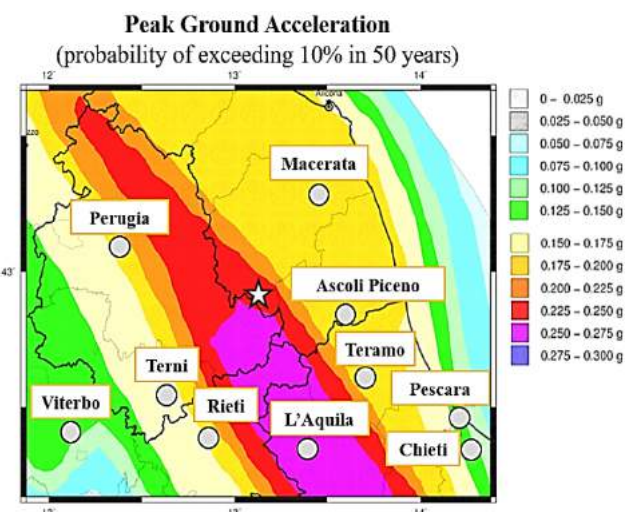
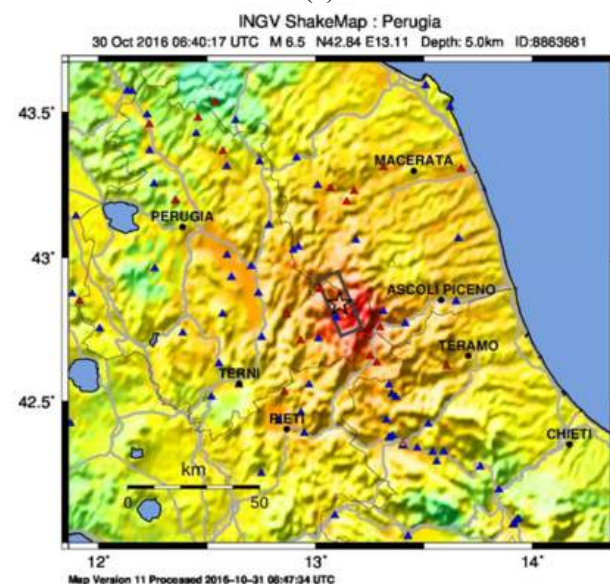
Two powerful replicas took place on October 26<sup>th</sup>, 2016 with epicentres at the Umbria-Marche border between the municipalities of Visso, Ussita and Castelsantangelo sul Nera with a magnitude of 5,9. On October 30<sup>th</sup>, 2016, the strongest shock, magnitude 6,5, with the epicenter between the municipalities of Norcia and Preci, in the Province of Perugia was recorded. The observations and preliminary analyses prepared by INGV [19] through seismological surveys, allowed a first interpretation of the event (Figure 3).



(a)



(b)



PERCEIVED SHAKING	Not felt	Weak	Light	Moderate	Strong	Very strong	Severe	Violent	Extreme
POTENTIAL DAMAGE	none	none	none	Very light	Light	Moderate	Mod./Heavy	Heavy	Very Heavy
PEAK ACC. (%g)	<0.06	0.2	0.8	2.0	4.8	12	29	70	>171
PEAK VEL. (cm/s)	<0.02	0.08	0.3	0.9	2.4	6.4	17	45	>120
INSTRUMENTAL INTENSITY	I	II-III	IV	V	VI	VII	VIII	IX	X+

Scale based upon Faenza and Michelini, 2010, 2011

(c)

Figure 3. Shake maps of the events occurred: (a) August 24<sup>th</sup>, 2016; (b) October 26<sup>th</sup>, 2016 and (c) October 30<sup>th</sup>, 2016 [19].

The seismogenetic area was characterized by the presence of different segments of fault with high structural complexity. The focal mechanisms (*slip*) allow identifying the type of movement that occurred following a specific earthquake, then how the area moved in response to tectonic deformation as reported in Fig. 4.



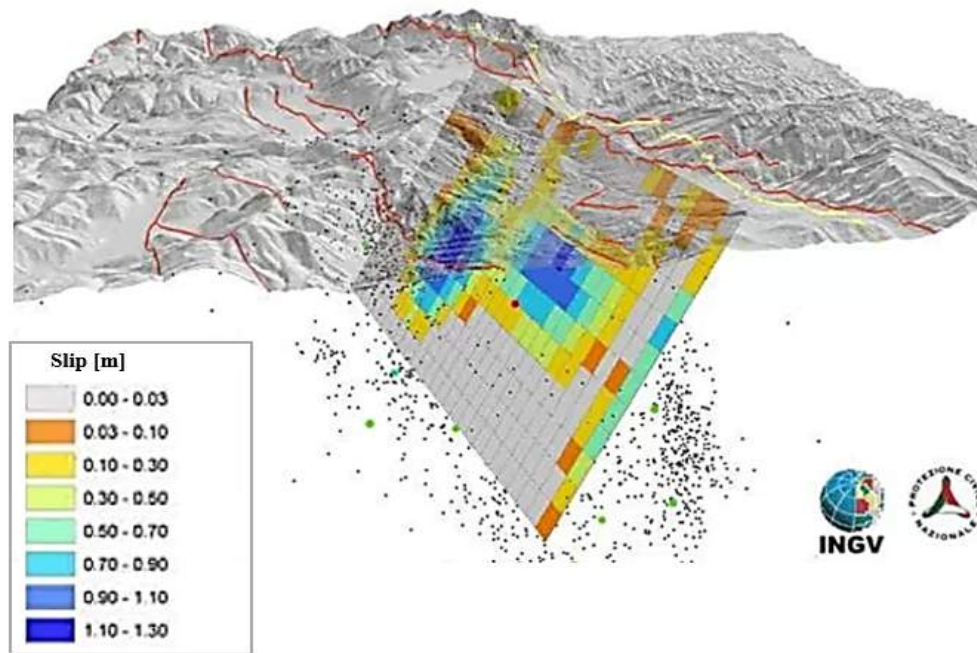


Figure 4. The focal mechanism occurred [19].

Already from the morning of August 24<sup>th</sup>, following the first excavations in the area, some surface fractures (cosmic effects) have been discovered and mapped [20], showing a continuity of at least 1,8 km from the Monte Vettore side. The maximum of cosismic deformation seems to be found near Accumoli (Fig. 5).

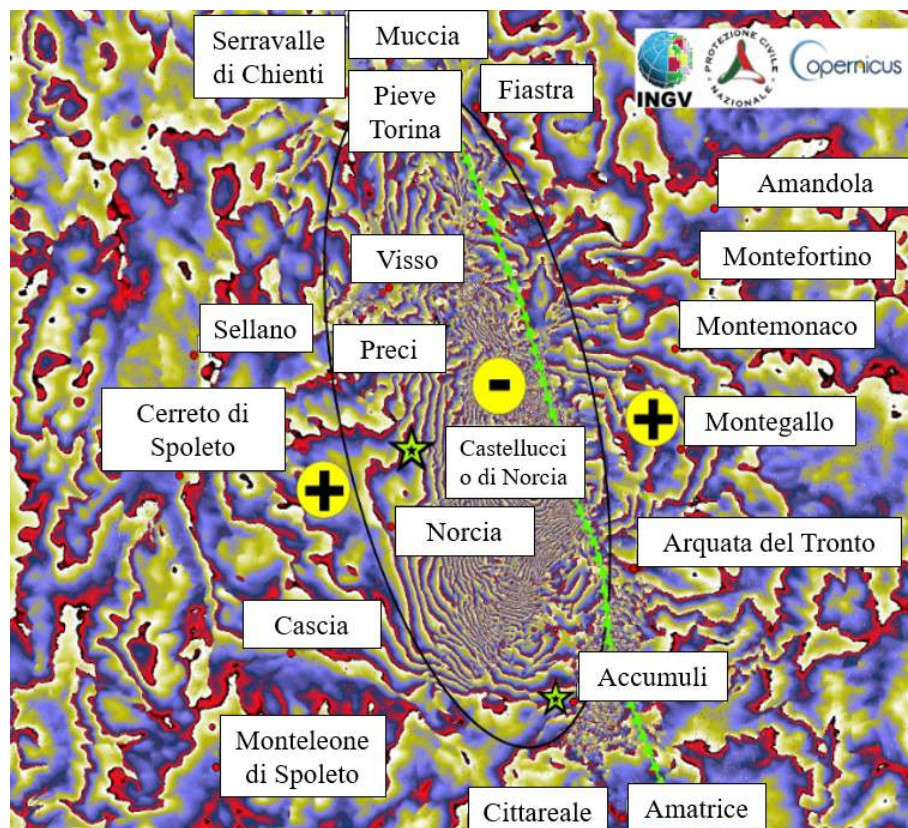


Figure 5. The coseismic deformation map [20].

The area was characterised by a vertical extension indicated with "+" in the previously figure, while, the zone subject to a depression, is indicated with the symbol "-". The green line indicates the seismic fault that generated the earthquake.

### 3. Seismic vulnerability assessment of the historical centre of Muccia

#### 3.1. Characterisation of the study area

The sub-urban sector analysed (Fig.6) is to be considered homogeneous from a typological and structural point of view. It consists of 50 masonry buildings dating back to the 19<sup>th</sup> century.



Figure 6. The sub-urban sector identification.

According to Building Typology Matrix (BTM) [21], this sector is composed by 50 buildings: M3.1 class masonry structures with steel floors (36% of the cases) and M3.3 class masonry structures with wooden floors (54%) and M3.4 masonry structures with rc floors (10%) (Fig.7).



## Typological Characterisation

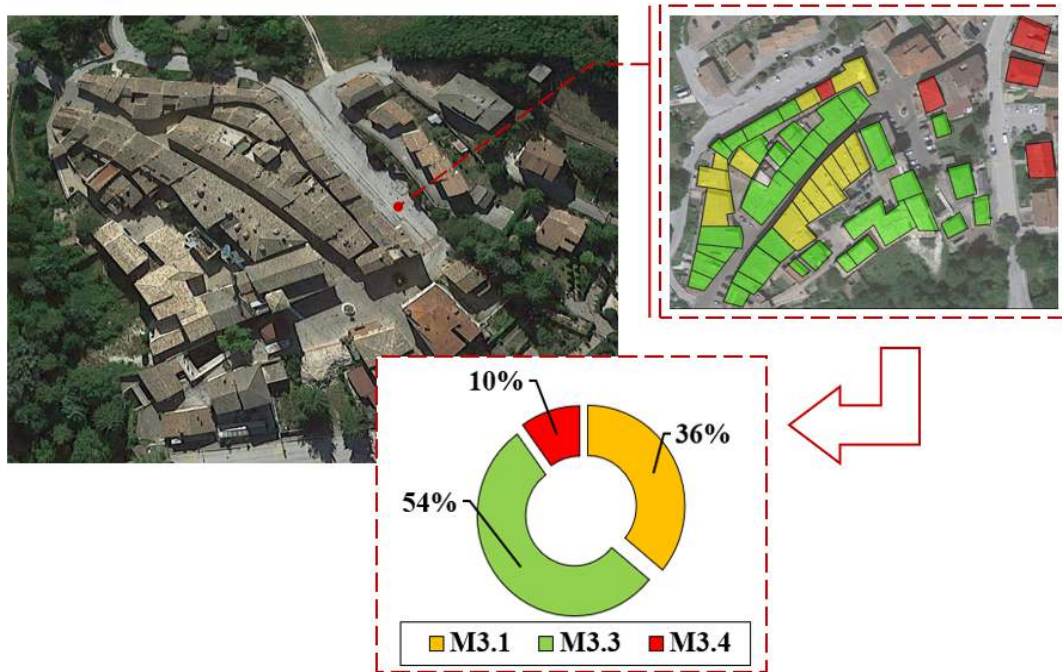


Figure 7. Typological characterisation of sub-urban sector.

The masonry aggregates under study generally develop in elevation from 2 to 3 stories. The inter-storey height is about 3.00-4.00 m for the first level and 3.00-3.50 m for other floors.

Roofing structures are often composed of double pitch r.c. beams with clay tile covering or wooden elements. In many cases the presence in the walls of an incongruous and brittle binder, which lost over time its characteristics, compromises the static nature of the buildings themselves and, sometimes, of the whole aggregate. The presence of these vulnerability factors increases the possibility of collapse and instability of the historical built-up when subjected to an impacting seismic action (Fig. 8).



Figure 8. Building conformation: a) vertical configuration; b) structural heterogeneities.

### 3.2. Seismic vulnerability assessment

Aiming at implementing a quick seismic evaluation procedure for masonry aggregates, it has been used the new vulnerability form proposed in Table 1 [22], which has been used in recent years for the seismic vulnerability assessment of several historical masonry aggregate [23, 24] (Table. 1).

Table 1. The vulnerability form for buildings in aggregate.

Parameters	Class Score, $S_i$				Weight, $W_i$
	A	B	C	D	
1. Organization of vertical structures	0	5	20	45	1,00
2. Nature of vertical structures	0	5	25	45	0,25
3. Location of the building and type of foundation	0	5	25	45	0,75
4. Distribution of plan resisting elements	0	5	25	45	1,50
5. In-plane regularity	0	5	25	45	0,50
6. Vertical regularity	0	5	25	45	0,50
7. Type of floor	0	5	15	45	0,80
8. Roofing	0	15	25	45	0,75
9. Details	0	0	25	45	0,25
10. Physical conditions	0	5	25	45	1,00
11. Presence of adjacent building with different height	-20	0	15	45	1,00
12. Position of the building in the aggregate	-45	-25	-15	0	1,50
13. Number of staggered floors	0	15	25	45	0,50
14. Structural or typological heterogeneity among adjacent S.U.	-15	-10	0	45	1,20
15. Percentage difference of opening areas among adjacent facades	-20	0	25	45	1,00

This new form is based on the method of the vulnerability index devised by Benedetti and Petrini [25]. This survey form is composed of 10 basic parameters and has been widely used in the past to survey the main structural system and the fundamental seismic deficiencies of isolated buildings in the case of an earthquake. In order to consider the structural interaction between adjacent buildings, not considered in the previously mentioned method, a new form has been adopted. The new form of investigation, appropriately conceived for the aggregates of masonry buildings, is conceived by adding five new parameters to the ten basic parameters of the original form. These new parameters take into account the interaction effects between the aggregate structural units under earthquake [26].

Formally, the methodology is based on the evaluation of a vulnerability index,  $I_v$ , for each S.U. of the aggregate intended as the weighted sum of the 15 parameters mentioned above. In Table 1, it is possible to notice how these parameters are distributed into four classes (A, B, C and D) with scores,  $S_i$ , of growing vulnerability.



A weight,  $W_i$ , is associated to each parameter that can range from 0,25 for the less important parameters to a maximum of 1,50 for the most important ones. According to this, the vulnerability index,  $I_v$ , can be calculated according to the following equation:

$$I_V = \sum_{i=1}^{15} S_i \times W_i \quad (1)$$

Subsequently,  $I_v$  is normalised in the range  $[0 \div 1]$ , adopting the notation  $V_I$ , by means of the following relationship:

$$V_I = \left[ \frac{I_V - (\sum_{i=1}^{15} S_{\min} \times W_i)}{\sum_{i=1}^{15} [(S_{\max} \times W_i) - (S_{\min} \times W_i)]} \right] \quad (2)$$

Based on these premises, the statistical distributions of the global vulnerability of the sub-urban sector analysed has been depicted in Figure 9.

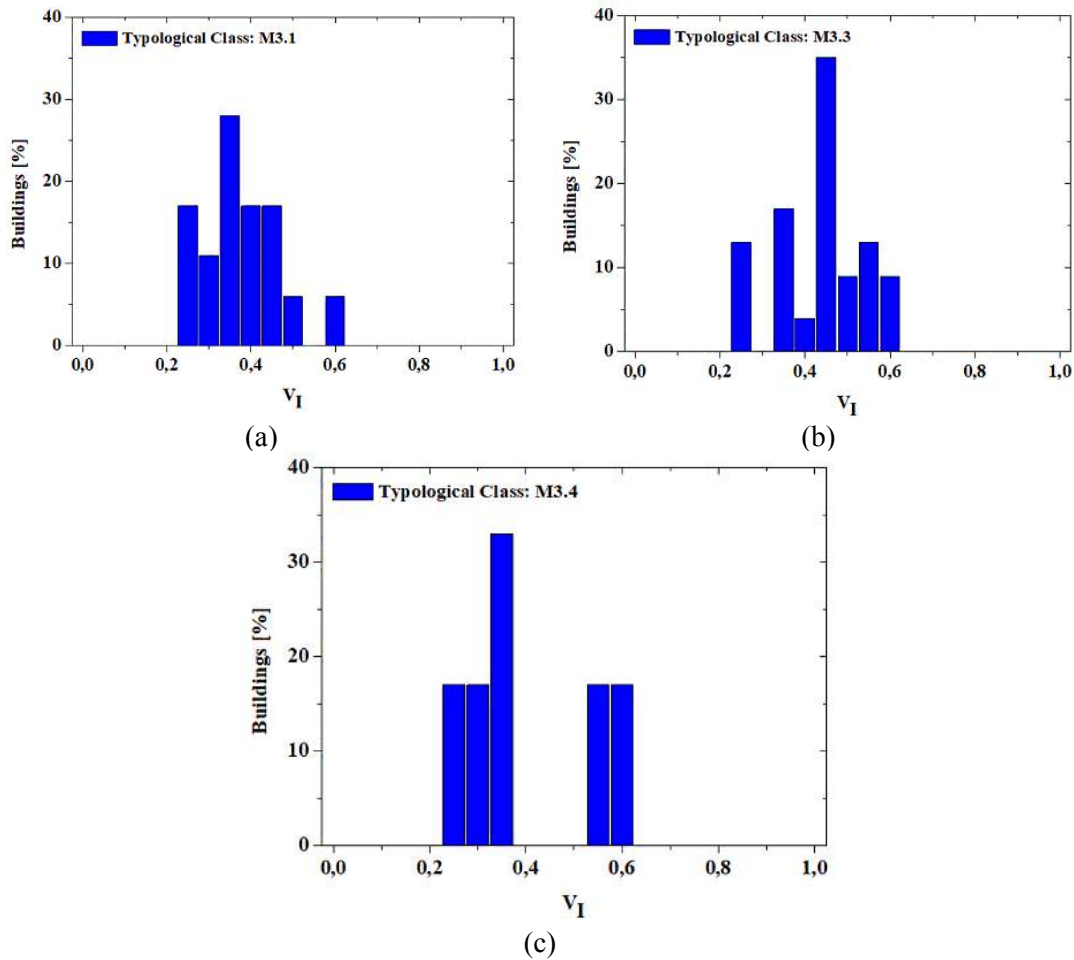


Figure 9: Vulnerability frequency distributions of the sample of buildings belonging to (a) M3.1, (b) M3.3 and (c) M3.4 typological classes.

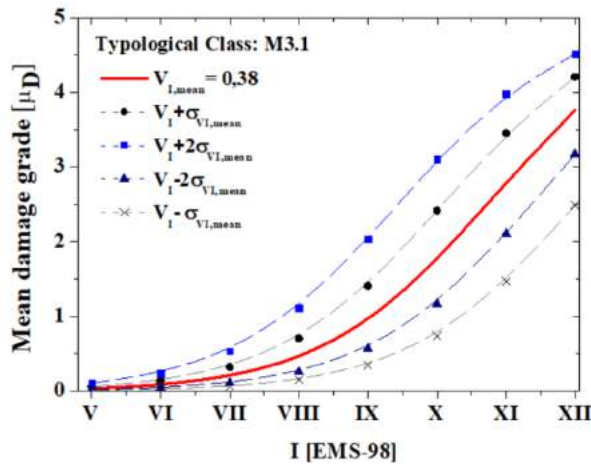
From the analysis of the results, it is worth noting how 28% of buildings belonging to the typological class M3.1 have a vulnerability index of 0,42 and only 5% have an index of 0,50 and 0,60. Similarly, for the class M3.3, 34% of the sample will have a vulnerability index of 0,42 and has a minimum of 3% associated with a vulnerability index of 0.38. Considering the M3.4 class, 35% of the buildings case have index of 0,38 and the 15% have index equal to 0,20 and 0,60, respectively.

### 3.3. Typological vulnerability curves

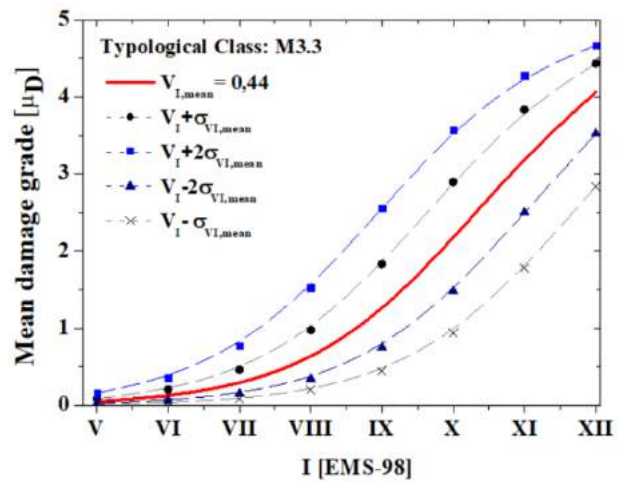
The proposed procedure, developed by [27], allows correlated macroseismic intensity, according to the EMS-98 scale, with the expected mean damage grade mathematically expressed by Eq. (3).

$$\mu_D = 2,5 \left[ 1 + \tanh \left( \frac{I + 6,25 \times V_I - 13,1}{Q} \right) \right] \quad (3)$$

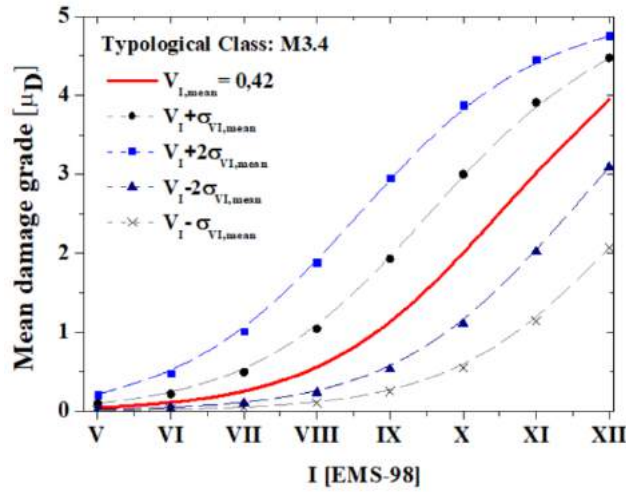
As can be seen, the vulnerability curves depend on three variables: the vulnerability index ( $V_I$ ), the hazard, expressed in terms of macroseismic intensity ( $I$ ), and a ductility factor  $Q$ , ranging from 1 to 4, which describes the ductility of typological classes of buildings and has been assumed as equal to 2,3 as proposed by [9]. The method refers to the vulnerability model implicitly included in the EMS-98 and accounts for the uncertainty in the attribution of the different building typologies to the EMS-98 vulnerability classes and for the variability in the building-to building vulnerability within the same typology. Therefore, the mean vulnerability curves shown in Figure 10 have been plotted in order to estimate the collapse probability of analysed buildings for different scenarios ( $V_I - \sigma_{V_I, Mean}$ ;  $V_I + \sigma_{V_I, Mean}$ ;  $V_I + 2\sigma_{V_I, Mean}$ ;  $V_I + 2\sigma_{V_I, Mean}$ ) [28, 29].



(a)



(b)



(c)

Figure 10: Mean typological vulnerability curves for the sample of buildings examined.

## 4 Estimated damage scenario

### 4.1 Damage model prediction

Scenario analysis allows to analyse in detail the damage associated with a generic structural system when subjected to a natural event. Referring to the case study examined, the damage associated with a seismic event is considered. In particular, according to the Section 2.1, a set of magnitudes, enclosed in the range [5,4 - 6,5] have been selected.

The severity of the damage was analysed thanks to predictive analysis in which, during the earthquake, buildings with the same structural characteristics would be subject to a damage that decreases when increase the epicentral distance. Subsequently, the attenuation law defines the macrosismic intensity according to EMS-98 by the formula proposed by Crespellani, [30] and reported in Equation (4).

$$I_{EMS-98} = 6,39 + 1,756M_w - 2,747 \times \ln(R + 7) \quad (4)$$

where,  $M_w$  is the moment magnitude occurred and  $R$  is the site-source distance expressed in Km. According to the scale EMS-98, six damage levels,  $D_k$ , each one associated to a damage score  $k$ , ranging from 0 to 5, are defined:  $D0$ : no damage;  $D1$  (*moderate damage*): with hair-line cracks in very few walls and fall of small pieces of plaster only;  $D2$  (*substantial damage*): structural damage and moderate non-structural damage. Cracks in many walls with fall of fairly large pieces of plaster. Partial collapse of chimneys;  $D3$  (*significant damage*): intensive structural damage and heavy non-structural damage, with large and extensive cracks in most walls; roof tiles detachment; chimneys fracture at the roof line; failure of individual non-structural elements (partitions, gable walls); activation of the first out-of-plane mechanisms;

*D4 (partial collapse)*: extended damage and very heavy non-structural damage, with serious wall failures; partial structural failure of roofs and floors; *D5 (collapse)*: collapse to both non-structural and structural parts, with total or near total collapse of the whole building. Considering the representative damage parameter  $\mu_D$ , the expected number of buildings that undergo a certain damage level has been determined (Fig. 11).

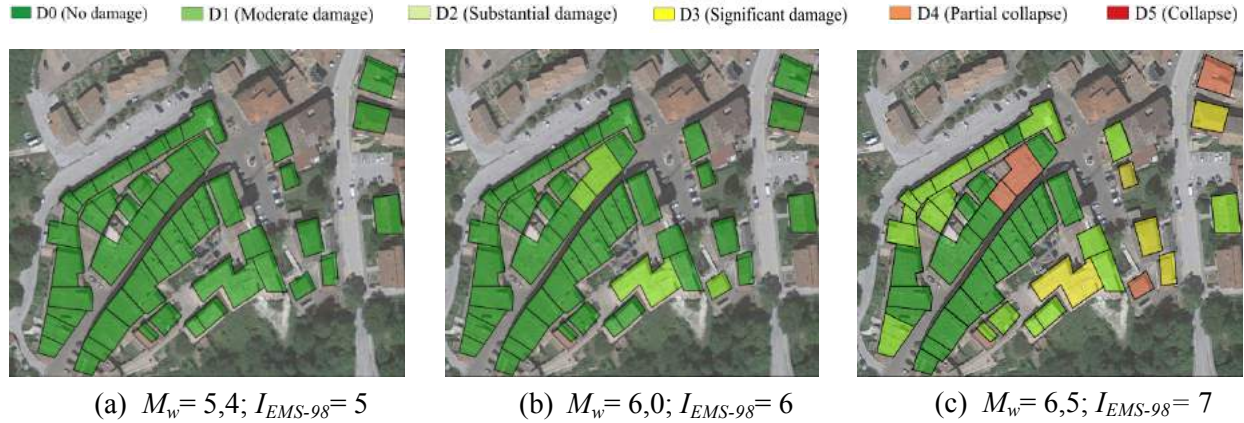


Figure 11. Damage scenarios for a set of moment magnitudes occurred.

A complete damage distribution has been defined from the scenario previously achieved. The conditional probability,  $P[D_k > D_i | M_w; R]$ , of exceeding a certain damage state,  $D_k$ , varying the magnitude,  $M_w$ , and epicentral distances,  $R$  were presented in Fig. 12.

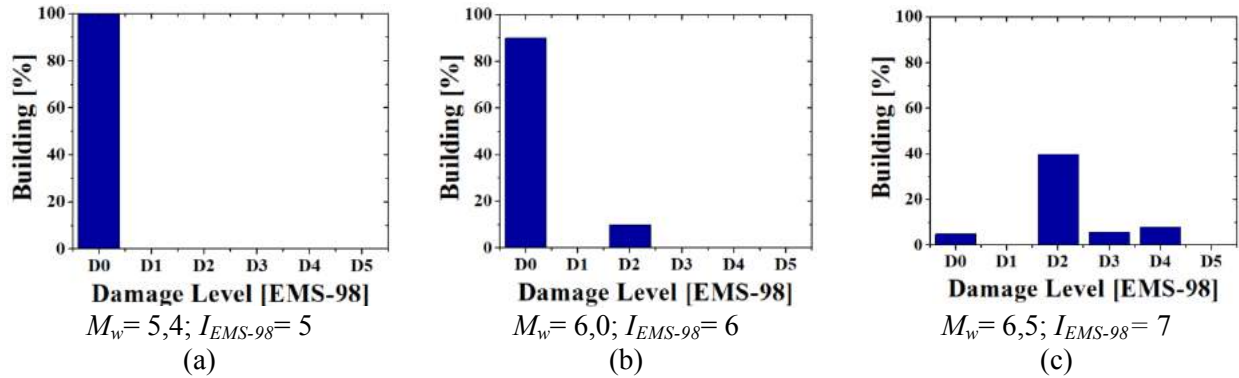


Figure 12. Vulnerability frequency distributions: (a) M3.1, (b) M3.3 and (c) M3.4 typological classes.

As can be seen, for a moment magnitude,  $M_w$ , equal to 5,4, a 100% of building stocks reached damage D0 (No Damage). Consequently, for a magnitude 6,0, the damage distribution shows that a 90% of the cases reached damage D0, instead only 10% of the sample are characterized by damage D2. Furthermore, referring to the event occurred on October 30<sup>th</sup> (epicenter at Accumuli), for a moment magnitude equal to 6,5, the damage distribution provided 40% of the buildings case suffered a D2 damage, 6% suffered a damage D3 and only the 8% of the buildings sample have D4 damage (Extended damage).



Moreover, considering the event occurred on October 30<sup>th</sup>, the correlation between the empirical damage scenario and site-inspection recognition have been showed in Fig.13.



Figure 13: Correlation between examined damage scenario and site-inspection.

## 4.2 Empirical fragility curves

Once the global vulnerability of the entire sub-sector under investigation was defined, it was possible to focus attention on the case study building indicated with the number 45 in the previous Section 3. The examined building is in an isolated position (Fig. 14). It is characterized by load-bearing masonry walls, with wooden floors and pitched roofs with an average height of 3.50 m.

The physical conditions denote a widespread damage characterized by the presence of cracks along the West and North façades, respectively.

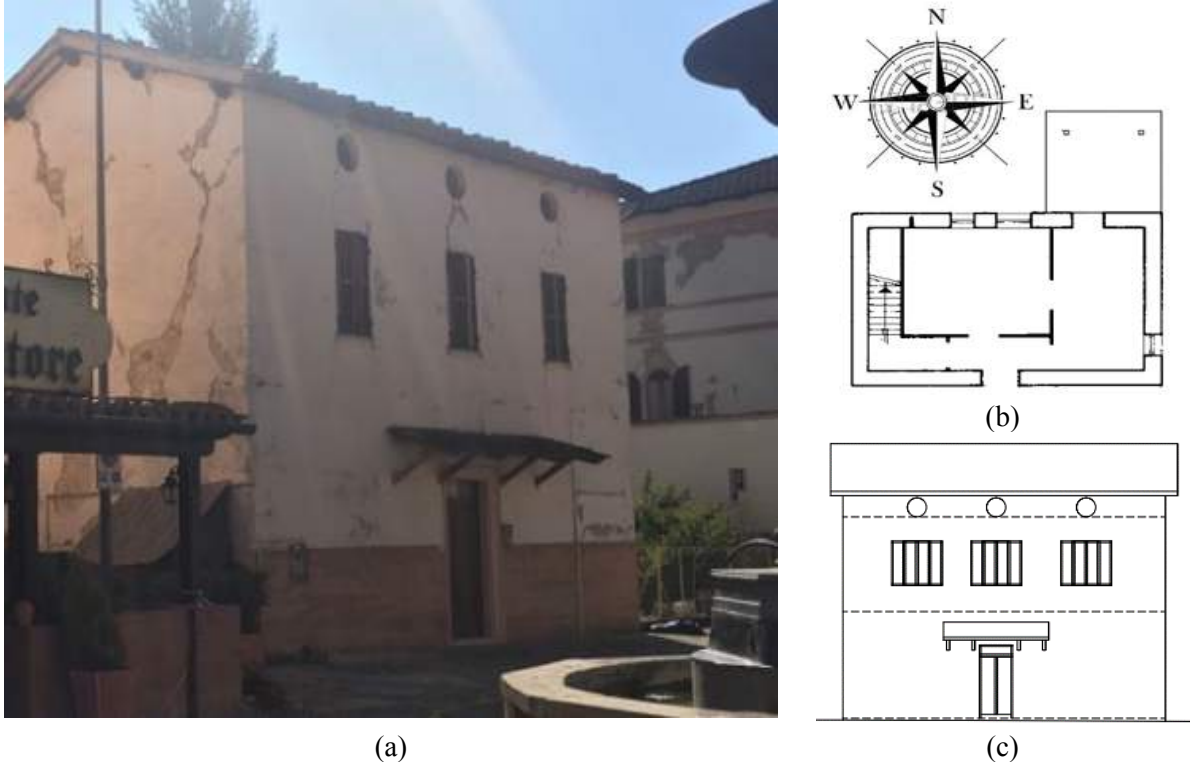


Figure 14: The case study building n.45, (a) street view, intermediate floor (b) and (c) North prospect.

The vulnerability index,  $V_L$ , derived from the index-based method for isolated buildings, is equal to 0,40. Fragility curves are used to define the probability of exceeding a certain degree of damage,  $D_k$  ( $K \in [0 \div 5]$ ). To this purpose, a correlation law proposed by Gaugenti-Petrini [31], is formally used in Equation (5).

$$\ln(PGA) = 0,602I - 7,073 \quad [g] \quad (5)$$

Mathematically, this law provides the variation of PGA as a function of macroseismic intensity,  $I$ , through empirical correlation coefficients  $C_1$  (0,602) and  $C_2$  (7,073). The gotten results are presented in Fig. 15.

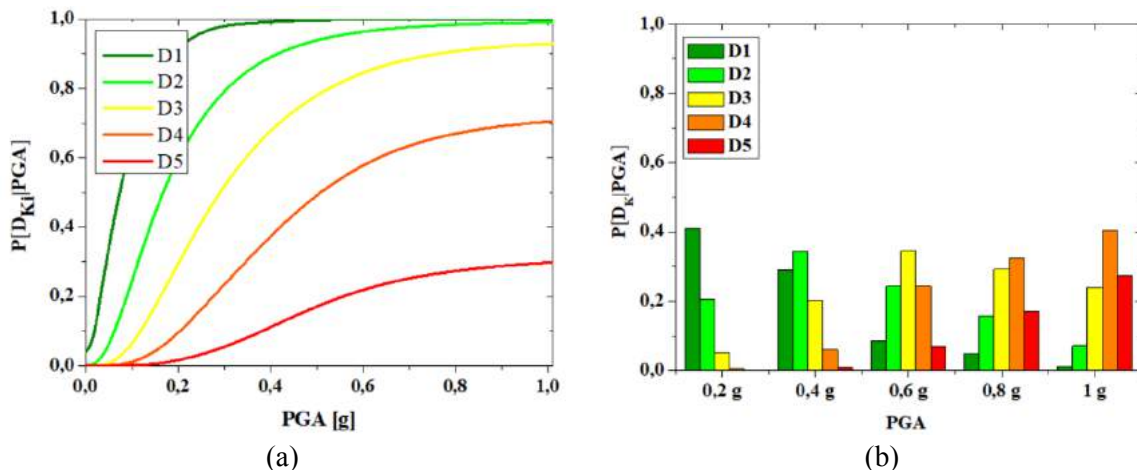


Figure 15: Fragility curves derived by empirical method (a) and damage distribution (b).

## 5 Mechanical vulnerability approach

### 5.1 Assessment of the structural properties

The mechanical characteristics of the materials were chosen according to Italian New Technical Codes for Constructions (NTC18) [32]. The masonry walls, both perimeter and internal, assume a constant thickness in height, without the presence of diffused heterogeneity. The mean compressive strength of masonry ( $f_m$ ) and shear strength ( $\tau_\theta$ ) are to be considered as minimum values of the range established by NTC18 referring to existing masonry buildings, respectively of 1,00 N/mm<sup>2</sup> and 0,02 N/mm<sup>2</sup>. The modulus of elasticity,  $E$ , have been considered of 870 N/mm<sup>2</sup>, likewise the tangential shear modulus,  $G$ , equal to 290 N/mm<sup>2</sup>. The specific weight of the masonry,  $W$ , is equal to 19,37 KN/m<sup>3</sup> as achieved in Table 2. Moreover, the mechanical properties of the timber elements (oak) are given in Table 3. The expected level of knowledge adopted is LC1 which corresponds to a reduction factor of the mechanical properties of the materials, F.C, equal to 1,35.

Table 2. Mechanical properties of masonry.

Mechanical Properties	Units	Masonry
Modulus of elasticity	$E$ (N/mm <sup>2</sup> )	870
Shear modulus	$G$ (N/mm <sup>2</sup> )	290
Mean compressive strength	$f_m$ (N/mm <sup>2</sup> )	1,00
Tensile strength	$\tau_\theta$ (N/mm <sup>2</sup> )	0,02
Specific weight	$W$ (Kg/m <sup>3</sup> )	1937

Table 3. Mechanical properties of wooden elements.

Mechanical Properties	Units	Timber
Modulus of elasticity	$E$ (N/mm <sup>2</sup> )	800
Shear modulus	$G$ (N/mm <sup>2</sup> )	590
Mean compressive strength	$f_m$ (N/mm <sup>2</sup> )	18
Tensile strength	$\tau_\theta$ (N/mm <sup>2</sup> )	3,5
Specific weight	$W$ (Kg/m <sup>3</sup> )	570

### 5.2 Non-linear static analysis

Non-linear static analysis have been performed by using 3Muri software developed by S.T.A. DATA srl [33]. About numerical modelling, according to the geometrical survey performed, the interstory height is assumed 3.50 m as resorting in the previous section. Wooden floors with thickness of 20 cm have been considered at each level.

Concerning the structural models, the structure is schematized through a series of macroelements interconnected to each other, in some cases leading towards the definition of the so-called "equivalent frames"[34, 35, 36, 37].

These macro-elements allow simulating the seismic behaviour of masonry structures, providing all the information required for their static linear analyses.

The 3Muri software uses macro-elements to generate the three-dimensional model of the structure, which is then automatically transformed into an assemblage of 3D equivalent frames to perform pushover analyses. The typical macro-element used for static linear analyses is schematised with the kinematic model reported in Figure 16 (a). The 3D model of the examined housing building, where it is apparent that masonry walls are modelled through a mesh of masonry piers and spandrels, is depicted in Figure 16 (b).

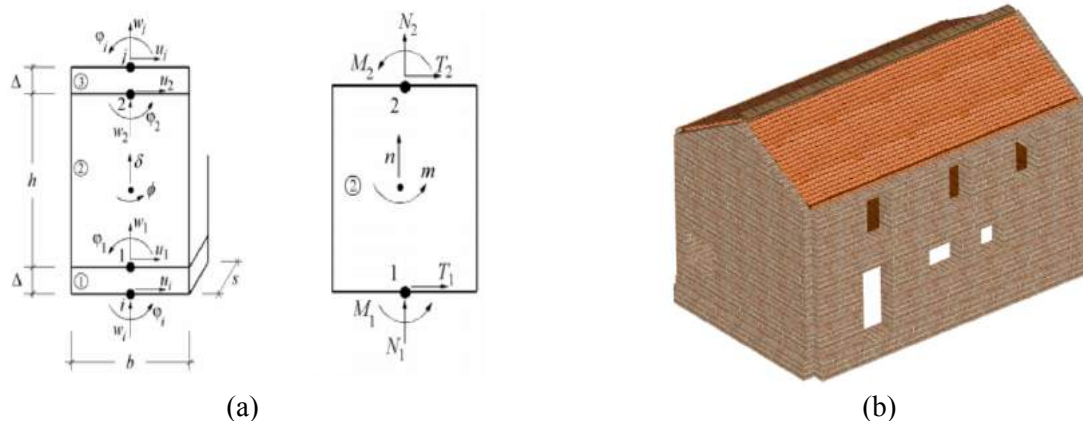


Figure 16: The macro-element kinematic model (a) and (b) the 3D building model with macro-elements through the 3Muri software.

The resistance criterias are given on the basis of EN 1998-3 [38] according to which the drift for shear and flexural crack mechanisms are established equal to 0.4% and 0.8% of the ultimate displacement ( $d_u$ ). The shear criteria is based on the diagonal cracks model and adapted to existing masonry buildings in the Italian seismic code, NTC18 [32]. The flexural response is developed by neglecting the tensile strength of the material and assuming a uniformly distributed compression stress distribution at the masonry interface.

Numerical analysis was performed considering a soil category “C” and a design spectrum referred to the Life Safety limit state. Dead and variable loads applied at the different structural levels, as well as partial safety factors for gravity loads combination at the Ultimate Limit State, are shown in Table 4.

Table 4. Design load applied.

Static Load	Intermediate Floor [KN/m <sup>2</sup> ]	Roof [KN/m <sup>2</sup> ]	Partial safety factor
$G_1$	3	3	1,3
$G_2$	2	1	1,3
$Q_k$	2	0,5	1,5



Non-linear static analysis has been performed in the two main directions (X and Y), taking also into account the effect of accidental eccentricities. The analysis results in terms of SDoF capacity curves and corresponding damage are shown in Figure 17.

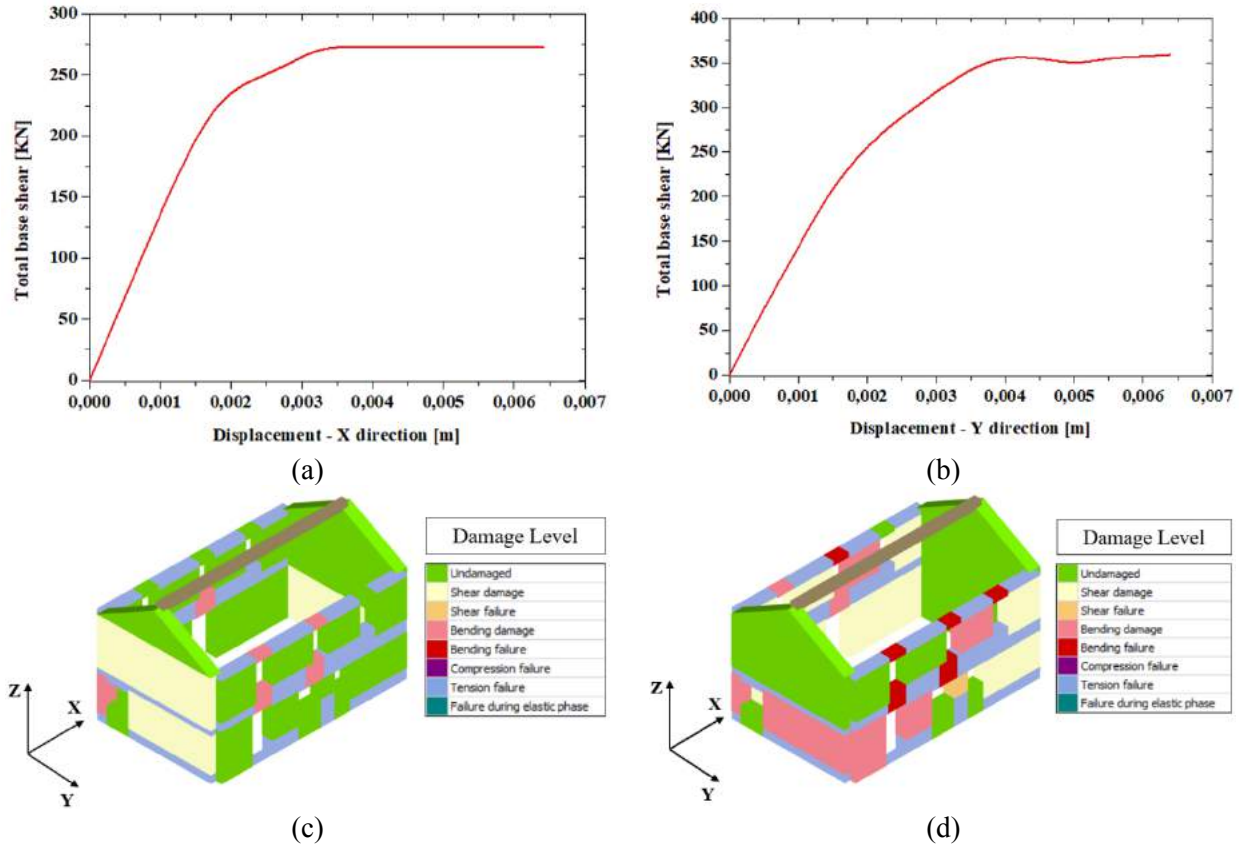


Figure 17: SdoF capacity curves: (a) X direction, (b) Y direction, (c) damage level in X direction and (d) damage level in Y direction.

The capacity curves show that in the  $X$  direction the structure has a maximum shear force equal to 272,66 kN with a yield displacement and ultimate displacements,  $D_y^*$  and  $D_u^*$ , equal to 0,0029 m and 0,0064 m, respectively. Similarly, in  $Y$  direction, the maximum shear threshold reached is 360,81 kN with the corresponding displacements equal to  $D_y^* = 0,0030$  m and  $D_u^* = 0,0065$  m.

Referring to a failure hierarchy, in  $X$  direction the distribution of ductile mechanisms (bending damage) occurs only in some masonry spandrels, whereas the fragile failures, induced by shear, are reached in the East and West façades, respectively. Moreover, the tensile failures are widespread (Figure 17 (c)). Similarly, in  $Y$  direction, the damage tends to increase globally. In fact, as can be seen in Figure 17 (d), bending failures occurred in the panel nodes instead the bending damage in some masonry panels. Concerning the shear damage, it is reached in the North and South façades, respectively. In terms of ductility ( $\mu$ ), in  $X$  direction the estimated value is 2,87 which corresponds to a percentage increment of 16,7% compared to the ductility calculated in the  $Y$  direction equal to 2,4.

The estimated vulnerability indices associated to the two main directions X and Y are evaluated as the ratio between the seismic demand and the corresponding capacity of the building considering the Ultimate Limite State (ULS). In particular, the calculated indexes, in X and Y direction, are 0,38 and 0,48, respectively.

### 5.3 Mechanical fragility curves

Fragility curves express the probability of exceeding a generic damage threshold,  $D_K$ , for a predetermined value of the Intensity Measurement ( $IM$ ), generally represented by the PGA or spectral displacements,  $S_d$ . The evaluation of the fragility curves is carried out according to the methodology proposed by [4]. In particular, four damage thresholds, D1 (slight), D2 (moderate), D3 (near collapse) and D4-D5 (collapse), have been defined and achieved in Table 4. As can be seen, the damage states are intrinsically defined considering the yielding displacement ( $D_y$ ) and ultimate displacement ( $D_u$ ) of the SDoF system.

Table 4. Damage thresholds.

Damage Limit State, $D_i$		Displacement Limit State
$D_1$	Slight	$0,7 D_y$
$D_2$	Moderate	$D_y$
$D_3$	Near collapse	$D_y + 0.5(D_u - D_y)$
$D_4-D_5$	Collapse	$D_u$

Methodologically, fragility curves are defined according to Equation (6)

$$P[D_K | PGA] = \Phi \left[ \frac{1}{\beta} \cdot \left( \frac{PGA}{PGA_{D_K}} \right) \right] \quad (6)$$

where,  $\Phi$ , is the cumulative distribution function,  $PGA_{D_K}$  is the median acceleration value associated for each damage threshold and  $\beta$  is the standard deviation of the log-normal distribution.

The dispersion,  $\beta$ , generally depends on the contribution of uncertainties in the seismic demand. This parameter is a function of the ductility,  $\mu$ , of the structural system intended as the ratio between ultimate displacement,  $D_u$ , and the corresponding yielding displacement,  $D_y$ . Based on this assumption, the estimate value of the disperisons are given in Table 5 [39].

Table 5. Standard deviation for each damage thresholds.

Standard Deviation, $\beta_i$		Ductility Limit State
$\beta_1$	Slight	$0,25+0,07\ln(\mu)$
$\beta_2$	Moderate	$0,2+0,18\ln(\mu)$
$\beta_3$	Near collapse	$0,1+0,41\ln(\mu)$
$\beta_4-\beta_5$	Collapse	$0,15+0,5\ln(\mu)$

However, in this research work, the fragility functions are derived according to Equation (7)

$$S_{a,e} = \omega^2 \cdot S_{d,e} = \left( \frac{2 \cdot \pi}{T} \right)^2 \cdot S_{D_K} \quad (7)$$

where,  $S_{ae}$  is the expected spectral acceleration,  $T$  is the vibration period of the structural system and  $S_{DK}$  is the spectral displacement associated to the damage thresholds reported in Table 4. Therefore, the fragility curves have been plotted in both directions, longitudinal X and transversal Y, respectively, and depicted in Figure 18.

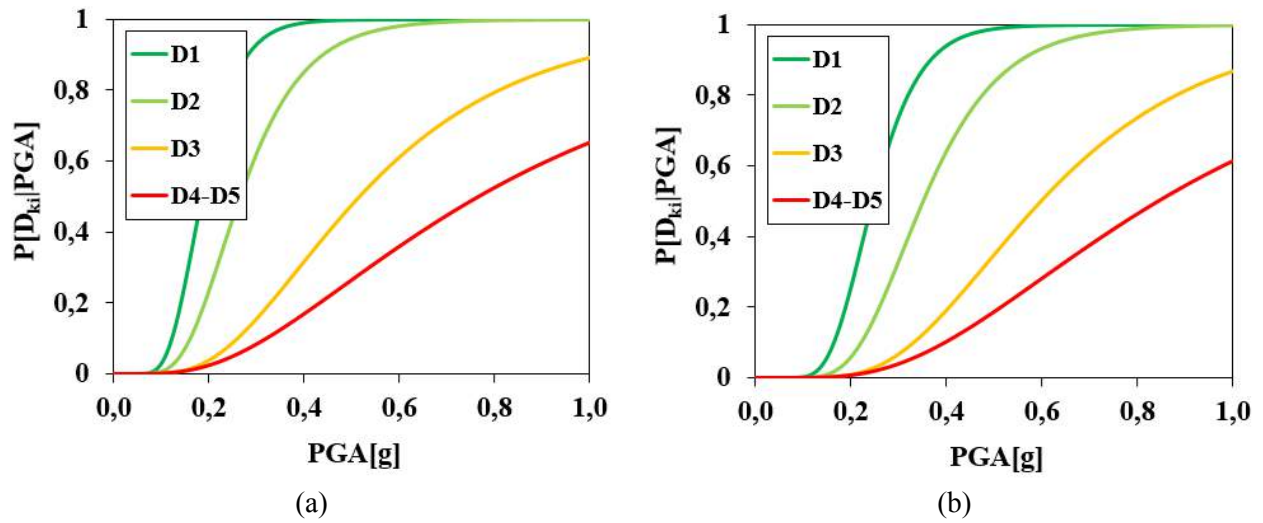


Figure 18: Fragility curves (a) X direction, (b) Y direction, respectively.

As analysed, it is possible to compare the fragility functions for the methods adopted in the present work. The gotten results are depicted in Figure 19.

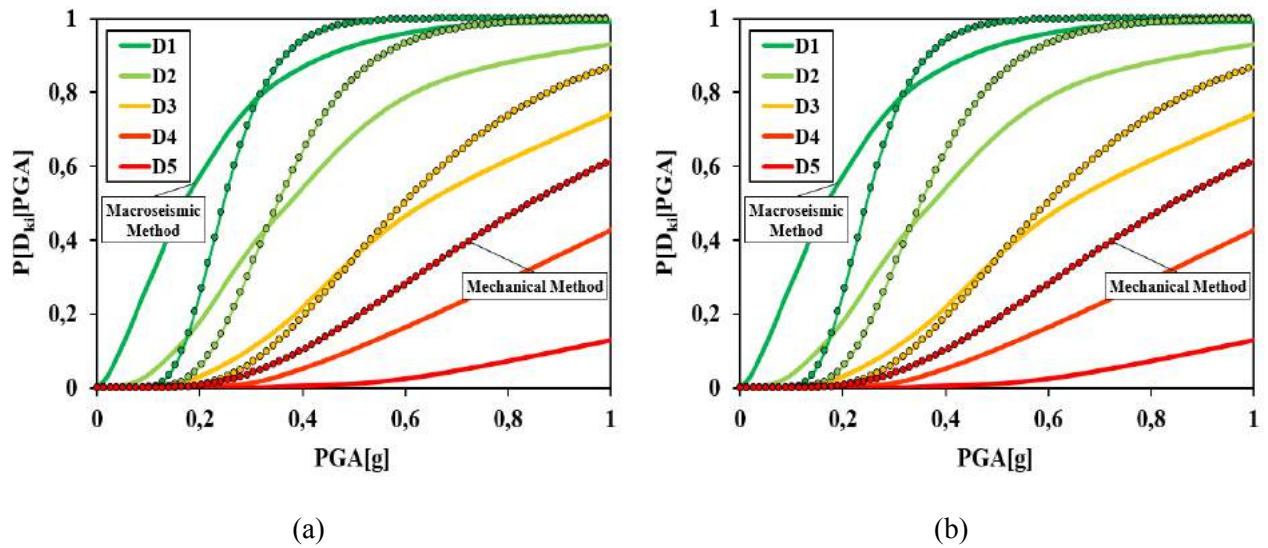


Figure 19: Fragility curves comparison: (a) X direction, (b) Y direction.

From the comparison of the applied methodologies, it is possible to notice how the fragility curves present different values of the expected damage.

Generally, this discrepancy is due the different procedures to estimate the damage threshold,  $D_K$ , and the uncertainties,  $\beta_i$ .

On one side, the macroseismic methodology, used for large-scale assessment, adopts an acceleration-intensity conversion law for the identification of the PGA range and, subsequently, it allows to plot the fragility curves through the cumulative distribution function without taking into account the uncertainties,  $\beta$ . On the other hand, the mechanical procedure provides more refined results since it takes into account the uncertainties of the structural system and combines them through the lognormal distribution.

Nevertheless, the macroseismic method in both analysis directions, tends to overestimate the damage thresholds  $D1$  and  $D2$  by 5% and 10%, respectively, for a spectral acceleration enclosed in the range  $[0 \div 0,3 \text{ g}]$ . Contrary, for PGA values greater than 0,3g, this method provides an underestimation for each damage levels considered. In particular, considering a damage  $D4$  and  $D5$  in both directions, it is possible to estimate a mean percentage decrease of 30% and 20%, compared to the mechanical procedure. As a conclusion, the mechanical approach can be considered as a very reliable tool in predicting fragility curves, since it provides safely more accurate results than the empirical method ones.

## 6 Conclusion

The study illustrates a comparison between two different approaches for estimating seismic vulnerability in terms of expected damage for an isolated masonry building located in the center of Muccia. The study area was composed by 50 structural units erected in aggregate, opportunely classified according to the BTM in three different classes as M3.1, M3.3, and M3.4, respectively. The assessment of seismic vulnerability of the inspected urban-sector has been analysed by means of index method approach. The statistical distribution of vulnerability indices shows, globally, a medium vulnerability of the stock.

Afterwards, mean typological vulnerability curves were derived in order to characterize the expected global damage varyinig the macroseismic intensity accoding to EMS-98 scale. The gotten results shown that, for seismic intensities less than X grade, the expected damage has not been relevant, but for high values of seismic intensity ( $X < I_{EMS-98} < XII$ ), the expected damage would cause an incipient collapse of the analysed sample.

Analysis of the damage scenario by means parametric approach have been considered using the attenuation law in terms of seismic intensity proposed by Crespellani.



Having defined a set of occurred magnitude ( $M_w$ ) and site-source distances ( $R$ ), it has been possible to analyse in detail the influence of these factors on an urban scale. The results obtained have shown that, the most severe scenario was for  $M_w=6,5$  in which at least 40% of the buildings reached damage D2 (Substantial damage) and 8% of the cases reached damage D4 (Extended damage).

Subsequently, an isolated building was considered as a case study. The mechanical approach was used for the characterisation of the structural model. A 3D model of the examined building, was modelled through a mesh of masonry piers and spandrels. The capacity of the structure in  $Y$  direction showed higher damage than the other orthogonal direction. In fact, considering a failure hierarchy a bending and shear damages tend to increase globally. In terms of ductility ( $\mu$ ), the results achieved shown an estimated value of  $\mu=2,87$  in  $X$  direction which corresponds to a percentage increment of 16,7% compared to the ductility calculated in the  $Y$  direction equal to 2,4. The vulnerability indices in  $X$  and  $Y$  directions, evaluated as the ration between the seismic demand and the capacity of the structure, were 0,38 and 0,48 respectively.

Consecutively, the fragility curves have been derived for both, empirical and mechanical approaches. From the comparison of the applied methodologies, the fragility curves present different values of the expected damage. Generally, these differences are due the different procedures to estimate the damage threshold,  $D_k$ , and the uncertainties,  $\beta_i$ . In particular, the macroseismic method in both analysis directions, tends to overestimate the damage thresholds by 5% and 10%, respectively, for a spectral acceleration enclosed in the range  $[0\div0,3 \text{ g}]$ .

Contrary, for PGA values greater than 0,3g, this method provides an underestimation for each damage levels considered of 30% and 20%, compared to the mechanical procedure. In conclusion, the macroseismic method can be considered an exhaustive approach for urban scale scenario analysis but its empirical nature tends to underestimate the damage compared to the mechanical ones. To improve the fragility curves, it will therefore be necessary to improve the estimation of the exposure at the time of the earthquake and to complete the observational database in order to ensure all the information on the surveyed buildings can be processed. For these reasons, the mechanical methodology used for estimating the expected damage through fragility curves, is a proven reliability method for the evaluation of seismic vulnerability.

## References

- [1] O.D. Cardona, M.K. van Aalst, J. Birkmann, M. Fordham, G. McGregor, R. Perez, R.S. Pulwarty, E.L.F. Schipper, B.T. Sinh, Determinants of Risk : Exposure and Vulnerability Coordinating, Managing the Risks of Extreme Events and Disasters to Advance Climate Change Adaptation. (2012). doi:10.1017/CBO9781139177245.005.
- [2] A.H. Barbat, M.L. Carreño, L.G. Pujades, N. Lantada, O.D. Cardona, M.C. Marulanda, Seismic vulnerability and risk evaluation methods for urban areas. A review with application to a pilot area, Structure and Infrastructure Engineering. (2010). doi:10.1080/15732470802663763.
- [3] R. Gonzalez-Drigo, A. Avila-Haro, A.H. Barbat, L.G. Pujades, Y.F. Vargas, S. Lagomarsino, S. Cattari, Modernist unreinforced masonry (URM) buildings of barcelona: Seismic vulnerability and risk assessment, International Journal of Architectural Heritage. (2015). doi:10.1080/15583058.2013.766779.
- [4] P. Lamego, P.B. Lourenço, M.L. Sousa, R. Marques, Seismic vulnerability and risk analysis of the old building stock at urban scale: application to a neighbourhood in Lisbon, Bulletin of Earthquake Engineering. 15 (2017) 2901–2937. doi:10.1007/s10518-016-0072-8.
- [5] P.B. Lourenço, J.A. Roque, Simplified indexes for the seismic vulnerability of ancient masonry buildings, in: Construction and Building Materials, 2006. doi:10.1016/j.conbuildmat.2005.08.027.
- [6] M.P. Ciocchi, S. Sharma, P.B. Lourenço, Engineering simulations of a super-complex cultural heritage building: Ica Cathedral in Peru, Meccanica. (2018). doi:10.1007/s11012-017-0720-3.
- [7] M. Angelillo, P.B. Lourenço, G. Milani, Masonry behaviour and modelling, in: CISM International Centre for Mechanical Sciences, Courses and Lectures, 2014. doi:10.1007/978-3-7091-1774-3\_1.
- [8] S. Tiberti, G. Milani, Historic city centers after destructive seismic events, the case of finale Emilia during the 2012 Emilia-Romagna earthquake: Advanced numerical modelling on four case studies, Open Civil Engineering Journal. (2017). doi:10.2174/1874149501711011059.
- [9] S. Lagomarsino, S. Giovinazzi, Macro seismic and mechanical models for the vulnerability and damage assessment of current buildings, Bulletin of Earthquake Engineering. (2006). doi:10.1007/s10518-006-9024-z.
- [10] S. Cara, A. Aprile, L. Pelà, P. Roca, Seismic Risk Assessment and Mitigation at Emergency Limit Condition of Historical Buildings along Strategic Urban Roadways. Application to the “Antiga Esquerra de L’Eixample” Neighborhood of Barcelona, International Journal of Architectural Heritage. 12 (2018) 1055–1075. doi:10.1080/15583058.2018.1503376.

- [11] F. Clementi, E. Quagliarini, F. Monni, E. Giordano, S. Lenci, Cultural Heritage and Earthquake: The Case Study of in Ascoli Piceno, *The Open Civil Engineering Journal*. (2017).  
doi:10.2174/1874149501711011079.
- [12] F. Clementi, V. Gazzani, M. Poiani, S. Lenci, Assessment of seismic behaviour of heritage masonry buildings using numerical modelling, *Journal of Building Engineering*. (2016).  
doi:10.1016/j.job.2016.09.005.
- [13] M. Valente, G. Milani, E. Grande, A. Formisano, Historical masonry building aggregates: Advanced numerical insight for an effective seismic assessment on two row housing compounds, *Engineering Structures* (2019), 190, 360-379.
- [14] S. Tiberti, M. Acito, M. Milani, Comprehensive FE numerical insight into Finale Emilia Castle behaviour under 2012 Emilia Romagna seismic sequence: damage causes and seismic vulnerability mitigation hypothesis, *Engineering Structures* (2016), 117, 397-421.
- [15] M. Valente, G. Milani, Damage assessment and collapse investigation of three historical masonry palaces under seismic actions (2019), *Engineering Failure Analysis*, 98, 10-37.
- [16] T.M. Ferreira, R. Maio, R. Vicente, Seismic vulnerability assessment of the old city centre of Horta, Azores: calibration and application of a seismic vulnerability index method, *Bulletin of Earthquake Engineering*. (2017). doi:10.1007/s10518-016-0071-9.
- [17] A. Basaglia, A. Aprile, E. Spacone, F. Pilla, Performance-based Seismic Risk Assessment of Urban Systems, *International Journal of Architectural Heritage*. 12 (2018) 1131–1149.  
doi:10.1080/15583058.2018.1503371.
- [18] G. Grünthal, (Ed.) *Chaiers du Centre Européen de Géodynamique et de Séismologie: Volume 15- European Macroseismic Scale 1998; European Center for Geodynamics and Seismology: Luxembourg, 1998; ISBN 2879770084*
- [19] D. Rapone, G. Brando, E. Spacone, G. De Matteis, Seismic vulnerability assessment of historic centers: description of a predictive method and application to the case study of scanno (Abruzzi, Italy), *International Journal of Architectural Heritage*. 12 (2018) 1171–1195.  
doi:10.1080/15583058.2018.1503373.
- [20] Savini Patrizio, *Storia della città di Camerino*, Second, Tipografia Sarli, 1864.
- [21] L. Chiaraluce, R. Di Stefano, E. Tinti, L. Scognamiglio, M. Michele, E. Casarotti, M. Cattaneo, P. De Gori, C. Chiarabba, G. Monachesi, A. Lombardi, L. Valoroso, D. Latorre, S. Marzorati, The 2016 Central Italy Seismic Sequence: A First Look at the Mainshocks, Aftershocks, and Source Models, *Seismological Research Letters*. (2017). doi:10.1785/0220160221.

- [22] INGV, Rapporto Di Sintesi Sul Terremoto in Centro Italia Mw 6.5 del 30 Ottobre 2016, Gruppo Di Lavoro INGV Sul Terremoto in Centro Italia. (2016) 1–49. doi:10.5281/zenodo.166019.
- [23] National Institute of Geophysics and Vulcanology, Prime interpretazioni dall’interferogramma differenziale ottenuto da dati radar del satellite europeo Sentinel-1, 2016. <https://ingvterremoti.wordpress.com>.
- [24] P. Mouroux, B. Le Brun, Presentation of RISK-UE project, Bulletin of Earthquake Engineering. (2006). doi:10.1007/s10518-006-9020-3.
- [25] A. Formisano, G. Florio, R. Landolfo, F.M. Mazzolani, Numerical calibration of an easy method for seismic behaviour assessment on large scale of masonry building aggregates, Advances in Engineering Software. (2015). doi:10.1016/j.advengsoft.2014.09.013.
- [26] N. Chieffo, A. Formisano, Geo-Hazard-Based Approach for the Estimation of Seismic Vulnerability and Damage Scenarios of the Old City of Senerchia (Avellino, Italy), Geosciences. 9 (2019) 59. doi:10.3390/geosciences9020059.
- [27] N. Chieffo, A. Formisano, The Influence of Geo-Hazard Effects on the Physical Vulnerability Assessment of the Built Heritage: An Application in a District of Naples, Buildings. 9 (2019) 26. doi:10.3390/buildings9010026.
- [28] D. Benedetti, V. Petrini, Sulla vulnerabilità sismica di edifici in muratura: Un metodo di valutazione, L’Industria Delle Costruzioni. (1984).
- [29] N. Chieffo, A. Formisano, T. Miguel Ferreira, Damage scenario-based approach and retrofitting strategies for seismic risk mitigation: an application to the historical Centre of Sant’Antimo (Italy), European Journal of Environmental and Civil Engineering. 0 (2019) 1–20. doi:10.1080/19648189.2019.1596164.
- [30] S. Lagomarsino, S. Giovinazzi, Macroseismic and mechanical models for the vulnerability and damage assessment of current buildings, Bulletin of Earthquake Engineering. 4 (2006) 415–443. doi:10.1007/s10518-006-9024-z.
- [31] T.M. Ferreira, R. Vicente, H. Varum, Seismic vulnerability assessment of masonry facade walls: Development, application and validation of a new scoring method, Structural Engineering and Mechanics. (2014). doi:10.12989/sem.2014.50.4.541.
- [32] R. Vicente, T. Ferreira, R. Maio, Seismic Risk at the Urban Scale: Assessment, Mapping and Planning, Procedia Economics and Finance. 18 (2014) 71–80. doi:10.1016/S2212-5671(14)00915-0.



- [33] T. Crespellani, C.A. Garzonio, Seismic risk assessment for the preservation of historical buildings in the city of Gubbio, in: *Geotechnical Engineering for the Preservation of Monuments and Historic Sites: Proceedings of the International Symposium on Geotechnical Engineering for the Preservation of Monuments and Historic Sites*, Napoli, Italy, 3-4 October 1996, 1997.
- [34] E. Guagenti, V. Petrini, The Case of Old Buildings: Towards a New Law - Intensity Damage, in: *Proceedings of the 12th Italian Conference on Earthquake Engineering—ANIDIS*. Italian National Association of Earthquake Engineering, Pisa, Italy (in Italian)., 1989.  
doi:10.1017/CBO9781107415324.004.
- [35] DM 17/01/2018, Aggiornamento delle “Norme Tecniche per le Costruzioni” - NTC 2018, (2018) 1–198.
- [36] S.T.A data srl, 3Muri 10.9.0 - User Manual, (n.d.).
- [37] Q. Piattoni, E. Quagliarini, S. Lenci, Experimental analysis and modelling of the mechanical behaviour of earthen bricks, *Construction and Building Materials*. (2011).  
doi:10.1016/j.conbuildmat.2010.11.039.
- [38] A. Formisano, Theoretical and Numerical Seismic Analysis of Masonry Building Aggregates: Case Studies in San Pio Delle Camere (L’Aquila, Italy), *Journal of Earthquake Engineering*. (2017).  
doi:10.1080/13632469.2016.1172376.
- [39] A. Formisano, Local- and global-scale seismic analyses of historical masonry compounds in San Pio delle Camere (L’Aquila, Italy), *Natural Hazards*. (2017). doi:10.1007/s11069-016-2694-1.
- [40] F. Clementi, A. Pierdicca, A. Formisano, F. Catinari, S. Lenci, Numerical model upgrading of a historical masonry building damaged during the 2016 Italian earthquakes: the case study of the Podestà palace in Montelupone (Italy), *Journal of Civil Structural Health Monitoring*. 7 (2017) 703–717. doi:10.1007/s13349-017-0253-4.
- [41] Eurocode 8, European Standard EN 1998-3:2005: Design of structures for earthquake resistance - Part 3: Assessment and retrofitting of buildings, Comité Européen de Normalisation, Brussels. (2005).
- [42] Z. V. Milutinovic, G.S. Trendafiloski, WP4: Vulnerability of current buildings. Risk-UE project Handbook, European Commission. (2003). doi:10.1007/978-1-4020-3608-8\_23.